Scientific paper

The Inhibition of Mild Steel Corrosion in 1 N HCl by Imidazole Derivatives

Niketan S. Patel,* Smita Jauhari and Girishkumar N. Mehta

Applied Chemistry Department, S V National Institute of Technology, Surat-395007, Gujarat, India

** Corresponding author: E-mail: niketan.ptl@gmail.com:*
Tel. /fax: +91 261 2201655

Received: 16-06-2009

Abstract

The inhibition effect of imidazole derivatives 4-methyl-2-propyl-1*H*-benzimidazole-6-carboxylic acid (MPBI) and 1,4'-Dimethyl-2'-propyl-1H,3'H-2,5'-dibenzimidazole (DPBI) against mild steel corrosion in 1 N HCl solutions were evaluated using conventional weight loss, potentiodynamic polarization, linear polarization and electrochemical impedance spectroscopy. The weight loss results showed that both are excellent corrosion inhibitors, electrochemical polarizations data revealed the mixed mode of inhibition and the results of electrochemical impedance spectroscopy have shown that the change in the impedance parameters, charge transfer resistance and double layer capacitance, with the change in concentration of the inhibitor is due to the adsorption of the molecule leading to the formation of a protective layer on the surface of mild steel. The inhibition action of these compounds was, assumed to occur via adsorption on the steel surface through the active centres contained of the molecule.

Keywords: Imidazole, Acid corrosion inhibitor, Electrochemical impedance spectroscopy, Mild steel

1. Introduction

Corrosion of iron and mild steel (MS) is a fundamental academic and industrial concern that has received a considerable amount of attention.[1] A study of the mechanism of the action of corrosion inhibitors has relevance both for the search for new inhibitors and for their effective use.[2] Huge amounts of acid solutions are used in the chemical industry to remove undesired scales and rust. The addition of corrosion inhibitors effectively secures the metal against an acid attack. Inhibitors are generally used in these processes to control metal dissolution[3] and, during the past decade, many organic inhibitors have been studied in different media.[4–7] The mechanism of their action can be different, depending on the metal, the medium or the structure of the inhibitor. One possible mechanism is the adsorption of the inhibitor blocking the metal surface thus hindering the corrosion process. Many N-heterocyclic compounds with polar groups and/or π-electrons are efficient inhibitors of the corrosion of steel and iron in acidic media.[8–11] This kind of organic molecules can adsorb on the metal surface because they form a bond between the N electron pair and/or the π-electron cloud and the metal thereby reducing the corrosive attack on metals in acidic media.[8]

The aim of this paper is to study the inhibiting action of new imidazole derivatives. The present work reports the use of imidazole derivatives 4-methyl-2-propyl-1*H*-benzimidazole-6-carboxylic acid (MPBI) and 1,4'-Dimethyl-2'-propyl-1H,3'H-2,5'-dibenzimidazole (DPBI) as corrosion inhibitors in 1 N HCl medium. Electrochemical behavior of MS in HCl media in the absence and in the presence of an inhibitor was studied using the mass loss method, potentiodynamic polarization, linear polarization and electrochemical impedance spectroscopy (EIS).

2. Experimental

2. 1. Inhibitor Preparation

Both the imidazole derivatives were synthesized according to a previously reported an experimental procedure.[12] The molecular formulas of imidazole derivatives are shown in Schema. 1. The choice of the compounds are based on molecular structure considerations; the presence of nitrogen atoms and aromatic rings is likely to facilitate the adsorption of the compound on the metal surface.

4-methyl-2-propyl-1*H*-benzimidazole-6-carboxylic acid (MPBI)

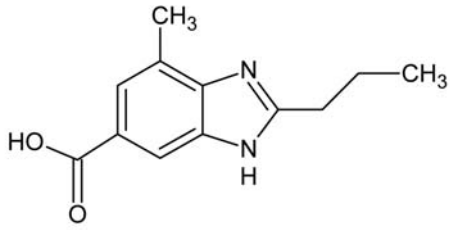

1,4'-Dimethyl-2'-propyl-1H,3'H-2,5'-dibenzimidazole (DPBI)

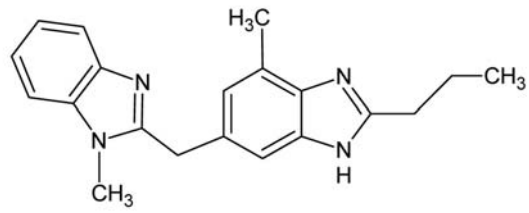

Schema 1. Chemical structures of imidazole derivatives

2. 1. 1. Process, Purity and Characterization of (MPBI & DPBI)

MPBI: A mixture of 7-methyl-2-propyl-3*H*-benzimidazole-5-carboxylic acid (10.0 g, 0.045 mol), *N*-methylbenzene-1, 2-diamine (8.0 g, 0.05 mol), and polyphosphoric acid (30.0 g) was heated at 150–155 °C for 4–5 h. The reaction mass was cooled to 70–80 °C and decomposed slowly with water (100 mL) at 70–80 °C. The pH of the reaction mass was adjusted to 4.5–5.0 using 20% NaOH solution, and the reaction mass continued stirring at the same temperature (70–80 °C) for 4–5 h to precipitate **1** as a crystalline solid. The crystalline solid obtained was filtered, washed thoroughly with water (50 mL), and then recrystallised from THF (90 mL) to obtain **1** in 11.7 g, 84% yield; mp 130–135 °C; MS *m*/*z* 305 (M+ + H); 1H NMR ($CDCl_3$) *ä* 7.8 (s, 1H), 7.2–7.7 (m, 6H), 3.89 (s, 3H), 2.80 (t, *J*) 7.4, 2H), 2.05 (s, 3H), 1.86 (q, *J*) 7.3, 2H), 0.99 (t, *J*) 7.4, 3H); 13C NMR (DMSO-*d*6) 13.7, 16.8, 21.0, 30.6, 31.7, 110.2, 113.4, 118.6, 121.7, 121.9, 122.9, 123.1, 136.6, 142.5, 154.3, 156.2.

DPBI: A solution of 4-butyrylamino-3-methyl-5-nitro benzene acid methyl ester (50.0 g, 0.178 mol), methanol (750 mL), and Pd-C (2.5 g) was placed in an autoclave system under hydrogen pressure (3.4 kg/cm^2) at 25–35 °C for 4 h. The reaction mass was filtered through a hyflowbed, and the catalyst was washed with methanol (100 mL). The combined filtrates were concentrated to obtain 42 g of as a thick residue. Water (400 mL) was added followed by sodium hydroxide (14.3 g, 0.357 mol) and heated to reflux temperature for about 5 h. After completion, the reaction mass was cooled to 25–35 °C, the pH of the reaction mass was adjusted to 4.5–5.0 using concentrated hydrochloric acid (34 mL), and then the reaction mass continued stirring for 45–60 min. The crystalline solid obtained was filtered, washed with water (200 mL), and dried at 55–60 °C for 2–3 h to obtain **2** as a white crystalline powder. Yield 36 g (92.54%); mp 295–297 °C; MS *m*/*z* 219 M+ + H; ^{1}H NMR ($CDCl_3$) 8.1 (s, 1H), 7.6–7.8 (m, 2H), 2.95 (t, *J*) 7.6, 2H), 2.90 (s, 3H), 1.90 (q, *J*) 7.5, 2H), 1.02 (t, *J*) 7.3, 3H).

Both these compounds are used as intermediates of sartan pharmaceuticals, especially for telmisartan and are non hazards.

2. 2. Preparation of Specimens

Cylindrical working electrodes of MS containing 0.09 % of P, 0.37 % of Si, 0.01 % of Al, 0.05 % of Mn, 0.19 % of C, 0.06 % of S, and the remainder of Fe were used for electrochemical polarization and impedance measurements. Surface preparation of mechanically polished specimens were carried out using different grades of emery papers, degreased with acetone, dried at room temperature and stored in a desiccator before use.

2. 3. Mass Loss Method

Polished and pre-weighed MS specimens were suspended in 100 mL test solutions, with different concentrations and without the inhibitor, for a fixed period of time; they were washed, dried and weighted. From the mass loss data, the percent inhibition efficiency (E_w %) was calculated.

2. 4. Electrochemical and Impedance Measurements

A three-electrode cell of borosil glass, consisting of a MS working electrode (WE), a pure platinum counter electrode (CE), and saturated calomel electrode (SCE) as the reference electrode, was used. The electrolytes used were acidic solutions maintained at 30 °C. The AC impedance measurements are shown as the Nyquist plots and polarization data as Tafel plots. A CH electrochemical analyzer model 608 C (USA) was used for this purpose. Polarization resistance measurements were carried out at the scan rate of 0.01 V s^{-1} at –10 mV to +10 mV versus the corrosion potential (E_{corr}) of the working electrode measured against SCE. Polarization curves were also obtained at the scan rate of 0.01 V s^{-1} in the range of –250 mV to +250 mV versus E_{corr}. Impedance measurements were carried out at the E_{corr}; 60 min after the electrode had been immersed in the test solution. The frequency range studied was 0.1 Hz to 1000 Hz. The AC signal was 5 mV peak-to-peak with 12 data points per decade.

3. Results and Discussion

The results of the mass loss measurements, the corrosion rates (W_{corr}) and the values of inhibition efficiency

(E_w%) for various concentrations of MPBI and DPBI after 2 h of immersion at 303K, 313K and 323K are given in Table – 1. The values of E_w% were calculated by the following equation:

$$E_W\% = 100 \times \frac{W_0 - W_{corr}}{W_0} \quad (1)$$

where W_{corr} and W_0 are the corrosion rates of MS with and without the additive respectively.

tion isotherm is applied to investigate the mechanism by the following equation:

$$\frac{C}{\theta} = \frac{1}{K} + C \quad (3)$$

Where C is the inhibitor concentration in the electrolyte and K is the equilibrium constant for the adsorption/desorption process.

Table 1: Inhibition Efficiency of MS in 1 N HCl in the presence and absence of different concentrations of MPBI and DPBI (Weight loss method)

Inhibitor		303 K		313 K		323 K	
	Concentration of inhibitor (ppm)	W (μg/cm² h)	Inhibition Efficiency E_W%	W (μg/cm² h)	Inhibition Efficiency E_W%	W (μg/cm² h)	Inhibition Efficiency E_W%
MPBI	0	13.06	–	14.91	–	15.52	–
	20	4.77	63	5.96	60	6.39	59
	40	3.93	70	5.36	64	5.89	62
	60	3.37	74	4.62	69	5.29	66
	80	2.75	79	3.75	75	4.62	70
	100	2.07	84	3.15	79	3.91	75
DPBI	0	11.96	–	12.95	–	14.16	–
	20	2.93	76	3.59	72	4.33	69
	40	2.07	82	3.01	77	3.91	72
	60	1.65	86	2.43	81	3.42	76
	80	1.37	89	2.08	84	2.79	80
	100	1.05	91	1.77	86	2.53	82

The degree of surface coverage θ for different concentrations of the inhibitor in acidic media has been evaluated from weight loss using the equation:

$$\theta = \frac{W_0 - W_{corr}}{W_0} \quad (2)$$

From Table-1, the increase of W_0 is more pronounced with the rise of temperature for the blank solution. In the presence of MPBI and DPBI θ decreases slightly with increasing experimental temperature, which could be caused by, desorption of the inhibitor from the steel surface. The slight decrease of θ suggests that the efficiency of MPBI and DPBI is independent of temperature. The result shows that MPBI and DPBI effectively protect the steel even at high temperature.

The adsorption of the inhibitor is influenced by the nature and the charge of the metal, the chemical structure of the inhibitor, distribution of the charge in the molecule, and the type of electrolyte.[13–17] Important information about the interaction between the inhibitor and steel surface can be provided by the adsorption isotherm. In the above work, it could be concluded that θ increases with the inhibitor concentration; this is attributed to more adsorption of inhibitor molecules onto the steel surface. Now, assuming that the adsorption of MPBI and DPBI belonged to the monolayer adsorption, then the Langmuir adsorp-

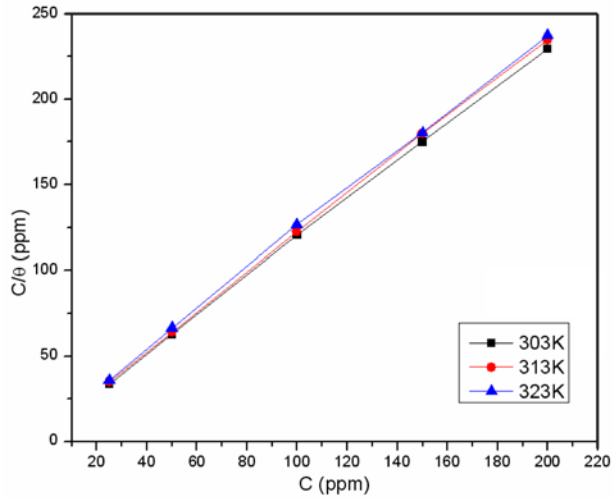

Figure 1. Langmuir adsorption plots for mild steel in 1N H_2SO_4 at different temperatures (MPBI)

Three representative Langmuir adsorption plots at different temperatures are shown in Fig. 1 and 2. Linear plots are obtained with slopes equal to 1.12, 1.14, 1.14 and 1.11, 1.13, 1.14 for MPBI and DPBI at the experimental temperature 303, 313 and 323 K, respectively. These results indicate that MPBI and DPBI occupies more than one adsorption site on the steel surface. A modi-

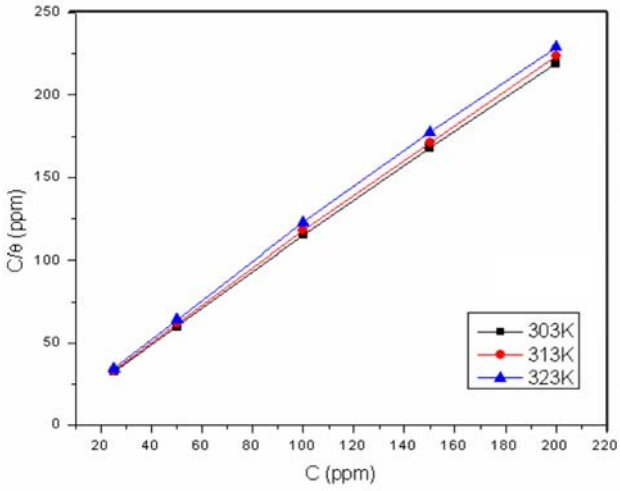

Figure 2. Langmuir adsorption plots for mild steel in 1N H_2SO_4 at different temperatures (DPBI)

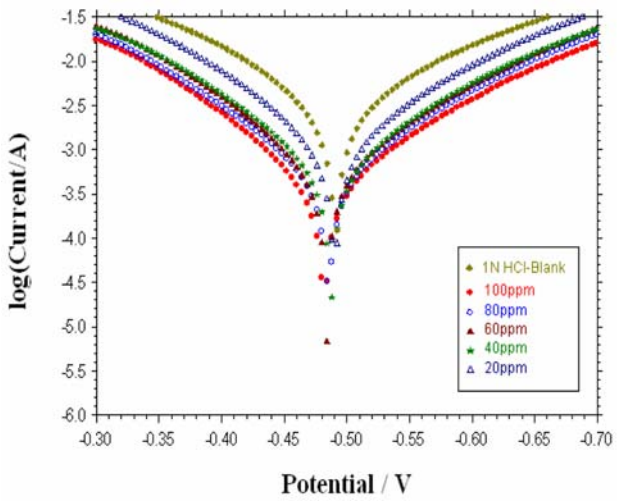

Figure 3. Tafel plots showing effect of MPBI on corrosion of MS in HCl medium

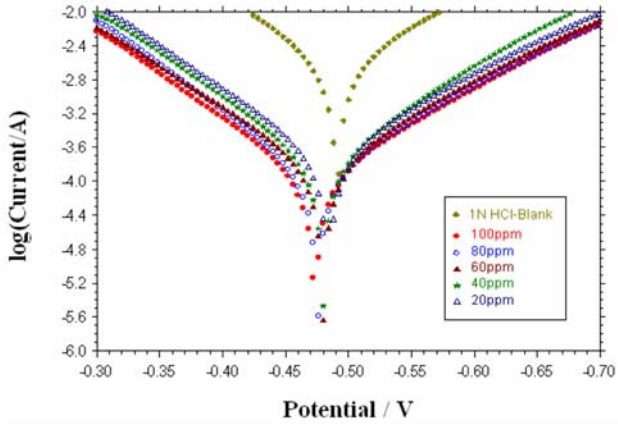

Figure 4. Tafel plots showing effect of DPBI on corrosion of MS in HCl medium

fied Langmuir adsorption isotherm[18–19] could be applied to this phenomenon, which is given by the corrected equation:

$$\frac{C}{\theta} = \frac{n}{K} + nC \tag{4}$$

Where n is the value of slopes obtained by above plot, The Langmuir isotherm, originally derived for the adsorption of gas molecules on solid surfaces, was modified to fit the adsorption isotherm of solutes onto solid surfaces in solution systems. The aim of this modification is based on the fact that direct application of the Langmuir isotherm to solution systems often leads to poor data fitting.

From the data in Table-1 it is clear that the value of E_w % increases with the increasing concentration of the inhibitor, suggesting an increase of the number of molecules adsorbed on the MS surface, blocking the active sites of acid attack and thereby protecting the metal from corrosion.

Potentiodynamic polarization data of various concentrations of MPBI and DPBI are shown as the Tafel plots for MS in 1 N HCl in Fig. 3 & 4. The corrosion kinetic parameters such as corrosion potential (E_{corr}), corrosion current density (I_{corr}), anodic and cathodic Tafel slopes (b_a and b_c) were derived from these curves and are given in Table-2. The values of inhibition efficiency (E_I %) were calculated using the following equation:

$$E_I\% = 100 \times \frac{I_{corr} - I_{corr(inh)}}{I_{corr}} \tag{5}$$

where I_{corr} and $I_{corr(inh)}$ are the values of corrosion current densities of MS without and with the additive, respectively, which were determined by extrapolation of the cathodic and anodic Tafel lines to the corrosion potential E_{corr}.

Inhibiting properties of the tested MPBI and DPBI were also evaluated by the determination of the polarization resistance. The corresponding polarization resistance (R_p) values of MS in 1 N HCl in the absence and the presence of the additives are given in Table-2. The inhibition efficiency (E_{Rp} %) was defined as follows:

$$E_{Rp}\% = 100 \times \frac{R_{P(inh)} - R_P}{R_{P(inh)}} \tag{6}$$

where R_p and $R_{p(inh)}$ are the polarisation resistance in the absence and in the presence of the inhibitor, respectively.

The data in Table 2 indicate that in both cases I_{corr} values gradually decreased with the increase of the inhibitor concentration with respect to the blank. Moreover, there was significant decrease in the values of both the anodic and cathodic tafel slopes with the increase in the inhibitor concentrations showing that the addition of the inhi-

Table 2: Effect of MPBI and DPBI on MS in 1N HCl media (electrochemical polarization studies)

Inhibitor	Concentration of inhibitor (ppm)	E_{corr} V	Tafel Constant (mV/decade) ba	bc	I_{corr} (mA/cm^2)	R_p (ohm cm^2)	E_I %	E_{Rp} %
MPBI	0	–0.4909	129	144	3.004	10	–	–
	20	–0.4900	105	119	1.100	22	63	55
	40	–0.4874	103	117	0.645	37	79	73
	60	–0.4838	98	116	0.554	42	82	76
	80	–0.4833	99	117	0.517	46	83	78
	100	–0.4821	97	117	0.392	59	87	83
DPBI	0	–0.4909	129	144	3.004	10	–	–
	20	–0.4838	98	118	0.206	113	93	91
	40	–0.4803	95	114	0.168	128	94	92
	60	–0.4798	99	116	0.152	157	95	94
	80	–0.4755	91	116	0.119	186	96	95
	100	–0.4732	95	116	0.114	200	96	95

bitor modifies the mechanism of the hydrogen reduction as well as decreases the rate of anodic dissolution up to good extent in both the cases. This means that MPBI and DPBI must have acted by blocking both the anodic and cathodic sites, so they behaved as mixed-type of the acid corrosion inhibitors.

The R_p values of MS in 1 N HCl in the absence and in the presence of different concentrations of the tested inhibitors are also given in Table 2. From these results it is clear that R_p values gradually increased with the increase of the inhibitor concentration. The values of inhibition efficiency of MPBI and DPBI obtained by electrochemical methods are in good agreement.

The corrosion behavior of MS in 1N HCl, in the absence and in the presence of various concentrations of MPBI and DPBI were also investigated by the EIS technique. The resultant Nyquist plots are shown in Fig. 5 & 6. The values of inhibition efficiency (E_R %) was calculated by the following equation:

$$E_R\% = 100 \times \frac{R_{t(inh)} - R_t}{R_{t(inh)}} \quad (7)$$

where R_t and $R_{t(inh)}$ are the charge-transfer resistance values in the absence and in the presence of the additives, respectively.

To obtain the values of double layer capacitance (C_{dl}), the values of frequency at which the imaginary component of the impedance is maximum $-Z_{im(max)}$ was found and used in the following equation with the corresponding R_t values:

$$C_{dl} = \frac{1}{2\pi f_{max} R_t} \quad (8)$$

The existence of a single semicircle in the Nyquist plot shows that there was only a single charge transfer process during the anodic dissolution of MS which remained unaffected in the presence of MPBI and DPBI added to the acid. An isolated Nyquist plot for the blank system is shown in the window in Fig. 5 and 6 and the value of real impedance (Z') was only 11 Ohms, which indicates the least charge transfer resistance (R_t) of the corrosion reac-

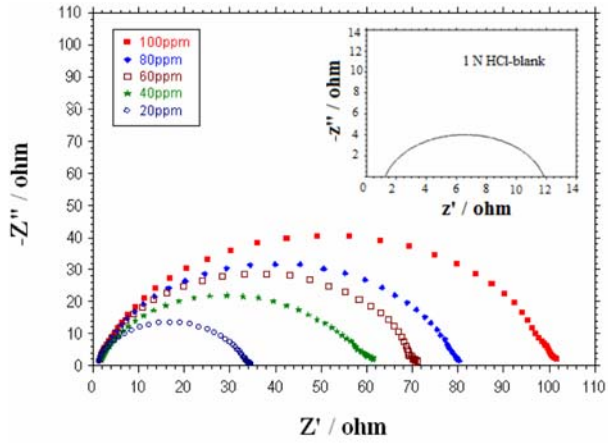

Figure 5. Nyquist plots showing effect of MPBI on corrosion of MS in HCl medium

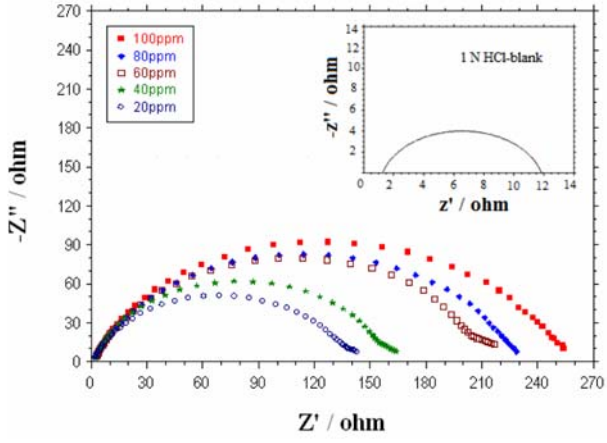

Figure 6. Nyquist plots showing effect of DPBI on corrosion of MS in HCl medium

tions. There was gradual increase in the diameter of each semicircle of the Nyquist plot when the concentration was increased from 20 to 100 ppm. This increase of the diameters clearly reflected that the R_t values also increased at the highest concentration of 100 ppm due to the formation and gradual improvement of the barrier layer of the inhibitive molecules, and as a result, the acid corrosion rate of MS gradually decreased.

Here, the frequency range employed was 0.1 Hz to 1000 Hz, in the Nyquist plot, real part (Z') was plotted on the x-axis and the imaginary part (Z'') on the y-axis of the chart. In Fig. 4 & 5, the low frequency data are on the right side of the plot and higher frequencies are on the left. Nyquist plots have one major shortcoming, at any data point on the plot, it cannot be told what frequency was used to record that point.

With the increase of the inhibitor concentration, the real impedance (Z') value increased as the R_t value increased. This can be understood by assuming that at the lower concentration of 20 ppm, the molecules was adsorbed on the metal surface partially and the major part of the surface remained unprotected; with an increase of the additive concentration, the number of molecules adsorbed on the metal surface increased and at the maximum concentration, the major part of the metal surface was covered.

Table-3 presents various parameters such as R_t and C_{dl}. There was a gradual decrease of the values of C_{dl} with the increase of the MPBI and DPBI concentration. The double layer between the charged metal surface and the solution is considered as an electrical capacitor.[20] The adsorption of the MPBI and DPBI on the electrode decreased its electrical capacity because they displaces water molecule and others ions originally adsorbed on the surface. The decrease of this capacity with the increasing MPBI and DPBI concentrations may be associated with the formation of a protective layer at the electrode surface. Inhibition efficiency was found to increase with the increasing MPBI and DPBI concentration. The results obtained from EIS show a similar trend as those obtained from electrochemical polarizations and mass loss measurements.

Table 3: Data from electrochemical impedance measurements of MS in 1 N HCl for various concentrations of MPBI & DPBI

Inhibitor	Concentration of inhibitor (ppm)	R_t Ohm cm^2	Cdl μF/cm^{21}	Inhibition Efficiency E_R (%)
MPBI	0	11	148.22	–
	20	34	135.89	68
	40	61	128.57	82
	60	71	115.23	85
	80	80	106.92	86
	100	101	90.60	89
DPBI	0	11	148.22	–
	20	145	92.20	92
	40	166	91.11	93
	60	218	90.50	95
	80	236	85.97	95
	100	265	83.59	96

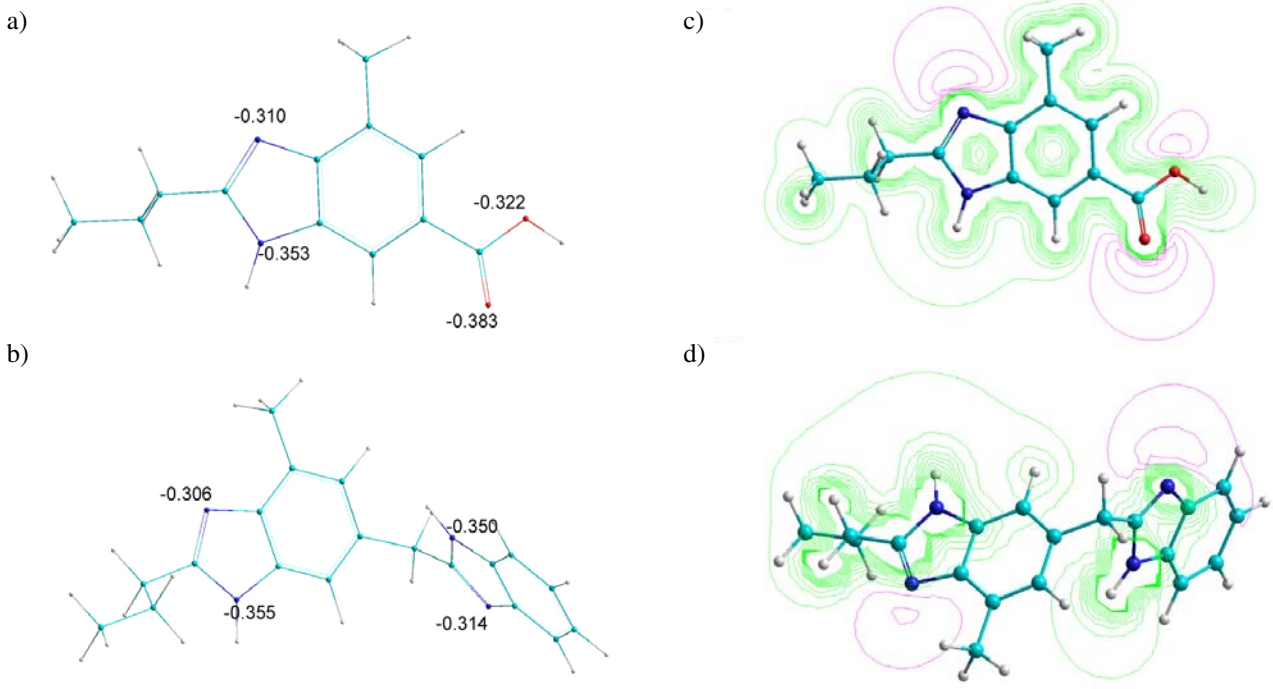

Figure 7. Semi-empirically optimized structure of MPBI (a) and DPBI (b), and the counter plot of their electrostatic potential (c) and (d) respectively.

MPBI and DPBI can be dissolved in HCl in the form of cations and anions. There are excess positive charges on iron surface at free corrosion potential.[21] Without the strong adsorbed anions on the metal surface; it is unfavorable for the adsorption of cations. In our experiment, for the anions it is very easy to adsorb on the electrode surface giving rise to a negative excess charges. Thus it is beneficial for cation adsorption. Moreover, according to molecular structure, there are few active adsorption centers on MPBI and DPBI, heteroatoms of N and O, all of them can contribute to the strong adsorption between inhibitor molecule and iron surface.

In order to get more information on the probable centre of adsorption, the structure of the organic inhibitors was optimized by applying semi-empirical method using RM1 (Recife Model 1) Hamiltonian.[22] RM1 is a recently developed semi-empirical molecular orbital model, capable of modeling most molecular systems of importance to organic chemistry, biochemistry and pharmaceutical research. This method is essentially identical to the AM1 method, but with improved performance, much newer and better parameters. RM1 yields superior results to both AM1 and PM3 methods for organic and bio-molecules. In the Fig. 7 the total partial atomic charges of more active atoms are given. And the counter plots shown in the red along in are more active zones to react with iron.

Analysis of the electrochemical data show that the inhibiting properties increase with inhibitor concentration. The inhibition efficiency increases in accordance to the order: DPBI > MPBI for all concentrations. Hence DPBI is better inhibitor than MPBI.

4. Conclusions

– The protection efficiency of these inhibitors increases with the increase of the inhibitor concentration; DPBI is better inhibitor than MPBI.
– Polarization curves showed that both MPBI and DPBI are mixed type inhibitors.
– The results of the weight loss, electrochemical polarization and EIS were all in very good agreement to support the above conclusions.

5. Acknowledgements

The authors thank Dr. P. D. Porey, Director and Dr. S Jauhari, Head of Applied Chemistry Department of S. V. National Institute of Technology, Surat for the scholarship, encouragement and facilities. Authors are thankful to Dr Suban K Sahoo for performing the quantum mechanical calculations.

6. References

1. H. H. Uhlig, R.W. Revie, Corrosion and Corrosion Control, Wiley, New York, **1985**.
2. G. Trabanelli, *Corrosion* **1991**, *47*, 410–419.
3. G. Schmitt, *Br. Corros. J.* **1984**, *19*, 165–176.
4. K. Tebbji, I. Bouabdellah, A. Aouniti, B. Hammouti, H. Oudda, M. Benkaddour, A. Ramdani, *Mat. Lett.* **2007**, *61*, 799–804.
5. F. Bentiss, F. Gassama, D. Barbry, L. Gengembre, H. Vezin, M. Lagrenee, M. Traisnel, *App. Surf. Sci.* **2006**, *252*, 2684–2691.
6. R. A. Prabhu, A. V. Shanbhag, T. V. Venkatesha, *J. Appl. Electrochem.* **2007**, *37*, 491–497.
7. G. Avci, *Colloids Surf. A-Physicochem. Eng. Aspects* **2008,** *317*, 730–736.
8. G. Trabanelli, in: Florain Mansfeld (Ed.), Chemical Industries: Corrosion Mechanism, Marcel Dekker, New York, **1987**.
9. S. Muralidharan, R. Charasekar, S.V.K. Iyer, *Proc. Indian Acad. Sci., Chem. Sci.* **2000,** *112*, 127–136.
10. F. Bentiss, M. Traisnel, M. Lagrenée, *Corros. Sci.* **2000**, *42*, 127–142.
11. Y. Yan, W. Li, L. Cai, B. Hou, *Electrochim. Acta* **2008**, *53*, 5953–5960.
12. K. S. Reddy, N. Srinivasan, C. R. Reddy, N. Kolla, Y. Anjaneyulu, S. Venkatraman, A. Bhattacharya, V. T. Mathad, *Org. Pro. Res. & Dev.* **2007**, *11*, 81–85.
13. A. Popova, E. Sokolova, S. Raicheva, M. Christov, *Corros. Sci.* **2003**, *45*, 33–58.
14. I. L. Rozenfeld, Corrosion Inhibitors, McGraw-Hill Inc., New York, 1981.
15. D. Zhang, L. Gao, G. Zhou, K. Lee, *J. Appl. Electrochem.* **2008**, *38*, 71–76.
16. J. Ueara, K. Aramaki, *J. Electrochem. Soc.* **1991**, *138,* 3245–3251.
17. I. Granese, *Corrosion* **1988**, *44***,** 322–327.
18. R. F. V. Villamil, P. Corio, J. C. Rubin, S. M. L. Agostinho, *J. Electroanal. Chem.* **2002**, *535* 75–83.
19. R. F. V. Villamil, P. Corio, J. C. Rubin, S. M. L. Agostinho, *J. Electroanal. Chem.* **1999**, *472* 112–119.
20. F. Bentiss, M. Lagrenée, M. Traisnel, J. C.Hornez, *Corros. Sci.* **1999**, *41*, 789–803.
21. K. YE, *Materials Protection* **1990**, *23***,** 37–45.
22. G. B. Rocha, R. O. Freire, A. M. Simas, J. J. P. Stewart, *J. Comput. Chem.* **2006**, *27*, 1101–1111.

Povzetek

Z meritvami izgube mase, potenciodinamične polarizacije, linearne polarizacije ter z elektrokemično impedančno spektroskopijo smo na jeklu v 1 M NaCl raziskovali protikorozivno delovanje derivatov imidazola (4-metil-2-propil-1*H*-benzimidazole-6-karboksilna kislina, MPBI; in 1,4'-dimethil-2'-propil-1H,3'H-2,5'-dibenzimidazol, DPBI). Ugotovili smo, da sta oba derivata odlična inhibitorja korozije. Iz eksperimantalnih podatkov lahko sklepamo, da se na površni kovine molekule derivatov imidazola adsorbirajo in s tem tvorijo zaščitno plast.